

Mobile Energy Requirements of the Upcoming NIST Post-Quantum Cryptography Standards

Markku-Juhani O. Saarinen

PQShield Ltd.

Oxford, United Kingdom

mjos@pqshield.com

Abstract—Standardization of Post-Quantum Cryptography (PQC) was started by NIST in 2016 and has proceeded to its second elimination round. The upcoming standards are intended to replace (or supplement) current RSA and Elliptic Curve Cryptography (ECC) on all targets, including lightweight, embedded, and mobile systems. We present an energy requirement analysis based on extensive measurements of PQC candidate algorithms on a Cortex M4 - based reference platform. We relate computational (energy) costs of PQC algorithms to their data transmission costs which are expected to increase with new types of public keys and ciphertext messages. The energy, bandwidth, and latency needs of PQC algorithms span several orders of magnitude, which is substantial enough to impact battery life, user experience, and application protocol design. We propose metrics and guidelines for PQC algorithm usage in IoT and mobile systems based on our findings. Our evidence supports the view that fast structured-lattice PQC schemes are the preferred choice for cloud-connected mobile devices in most use cases, even when per-bit data transmission energy cost is relatively high.

Index Terms—Post-Quantum Cryptography, Energy Efficiency, Cortex M4, Mobile Cloud

I. INTRODUCTION

Vulnerability of factoring-based and (elliptic curve) discrete logarithm cryptography (RSA, DL, ECDL, ECC) to quantum computing has been known since Shor published his celebrated algorithm in 1994 [1]. The following 25 years have seen several breakthroughs and a steady improvement in the capabilities of quantum computers – but also the emergence and maturing of the field of Post-Quantum Cryptography (PQC) which studies public-key algorithms that are resistant to attacks by quantum computers in addition to classical threats.

The first dedicated PQCrypto workshop in 2006 already featured talks about lattice-based, hash-based, code-based, and multivariate cryptography [2]. These remain the major groups of post-quantum algorithms 14 years later, with the addition of the isogeny problem of supersingular curves [3], [4].

As quantum-safe “drop-in replacements” to RSA and ECC, post-quantum cryptography does not have the practical limitations of Quantum Key Distribution (QKD) and other solutions that do not support the public-key model and impose strict physical requirements on the transmission channel [5].

As shown in this work, established PQC proposals include public-key encryption and signature algorithms that require

less computational resources than RSA or ECC and are therefore suitable replacements in handheld devices, smart cards, and Internet-of-Things (IoT) applications. There are also PQC proposals that are prohibitively “heavy” for any of these targets, so understanding the individual characteristics of each algorithm is necessary for system design.

A. Post-Quantum Standardization and Transition

In August 2015 the U.S. Committee for National Security Systems (CNSS) and National Security Agency (NSA) announced “plans for transitioning to quantum-resistant algorithms” in National Security Systems (NSS), i.e. all governmental systems that handle classified information [6], [7].

Standardization bodies such as ETSI (European Telecommunications Standards Institute) had already initiated studies of quantum-safe cryptography with the view on standardizing it [8], but the 2015 CNSS/NSA post-quantum transition announcement created an immediate requirement for U.S. NIST (National Institute for Standards and Technology) to start a competitive standardization effort for U.S. Government use.

NIST has studied quantum-resistant cryptography at least since 2009 [9]. The current NIST PQC project is widely seen as a successor to previous, highly influential standard-selection competitions that led to the development of AES (Advanced Encryption Standard project, 1997–2001 [10]) and SHA-3 (Secure Hash Algorithm project, 2007–2012 [11]).

The NIST PQC algorithm requirements were released in late 2016 and initial submissions were due 30 November 2017, with 69 proposals entering the competition. In two years the effort has proceeded to its second selection round with 26 proposals remaining, out of which 17 are for encryption and key encapsulation (KEM) and 9 are intended for signatures [3], [12]. Table I lists current candidates along with their rough classification and also whether or not they had suitable lightweight implementations for this study (“PQPS”).

The NIST PQC project will go through a third elimination round in 2020/2021, but we already can have a fair understanding of the relative computational and communication requirements of the future standards – it is expected that more than one of the current candidates will be standardized and these algorithms will gradually replace RSA and ECC in applications. Previous experience indicates that such algorithm transitions typically take at least a decade to complete.

TABLE I
SECOND ROUND NIST PQC CANDIDATE ALGORITHMS.

Name	Type	Family	Problem	PQPS
BIKE	KEM	Codes	QC-MDPC	–
Classic McEliece	KEM	Codes	Goppa	–
DILITHIUM	Sign	Lattice	Fiat-Shamir	✓
Falcon	Sign	Lattice	Hash&Sign	✓
FrodoKEM	KEM	Lattice	LWE	✓
GeMSS	Sign	Multivar.	HFE	–
HQC	KEM	Codes	QCSD	–
KYBER	KEM	Lattice	MLWE	✓
LAC	KEM	Lattice	RLWE	✓
LEDAcrypt	KEM	Codes	QC-LDPC	–
LUOV	Sign	Multivar	UOV	–
MQDSS	Sign	Multivar.	Fiat-Shamir	–
NewHope	KEM	Lattice	RLWE	✓
NTRU	KEM	Lattice	NTRU	✓
NTRU Prime	KEM	Lattice	NTRU	–
NTS-KEM	KEM	Codes	Goppa	–
Picnic	Sign	Symmetric	ZKP	–
qTESLA	Sign	Lattice	Fiat-Shamir	–
Rainbow	Sign	Multivar.	UOV	–
ROLLO	KEM	Codes	Low Rank	–
Round5	KEM	Lattice	LWR/RLWR	✓
RQC	KEM	Codes	Low Rank	–
SABER	KEM	Lattice	MLWR	✓
SIKE	KEM	Isogeny	Supersingular	✓
SPHINCS+	Sign	Symmetric	Hash	–
Three Bears	KEM	Lattice	IMLWE	✓

B. NIST: PQC Key Establishment and Signatures Only

The 2016 NIST call for candidate algorithms [13] limited the competition to three types of public-key primitives: Key Encapsulation Mechanisms (KEMs), public key encryption algorithms, and digital signature algorithms. KEMs and public key encryption algorithms can be trivially converted into each other – KEM was originally proposed as a “better way of doing public-key encryption” [14]. KEMs can also be used for (ephemeral) key exchange and key establishment, although they may lack commutative and contributory properties of Diffie-Hellman required by some protocols [15].

NIST defines five security levels for post-quantum algorithms; these correspond to best classical and quantum attacks that can be mounted against AES-128 (L1), SHA-256 (L2), AES-192 (L3), SHA-384 (L4), and AES-256 (L5). The best classical attacks against AES and SHA are traditional brute-force and birthday attacks so L1/L2 has 128-bit, L3/L4 has 192-bit, and L5 has 256-bit classical security (in addition to being quantum-secure). The quantum security of L1, L3, and L5 is determined via Grover’s [16] algorithm. For Levels L2 and L4 quantum collision attacks [17] can be used.

We observe that the external functionality provided by NIST PQC algorithms closely matches NIST’s current RSA and ECC-based public-key standards, namely SP 800-56 [18], [19] for key establishment and FIPS 186-4 [20] for digital signatures. A far wider spectrum of quantum-secure schemes exists; especially hard lattice problems allows construction of virtually any type of scheme, from Identity- and Attribute-based Encryption (IBE and ABE) to Fully Homomorphic Encryption (FHE) [21].

C. Hybrid and Dual PQC Schemes

Conservative early adopters of PQC cryptography may first adopt a hybrid (dual, composite) approach to both key establishment and digital signatures. In such a scheme a PQC primitive is coupled with a conventional public-key algorithm for additional security assurance or interim FIPS 140 compliance before NIST PQC algorithms are fully approved.¹

Newly designed systems will probably skip the hybrid stage as it effectively doubles the engineering effort and has a severe negative impact on computational overhead – with conventional public-key cryptography often being the performance bottleneck. The main hybrid approaches are:

1) *Hybrid Key Establishment*: It is possible to design a hybrid key establishment method that uses a PQC algorithm in conjunction with a conventional method such as ECDH (Elliptic Curve Diffie-Hellman) in such a way that *both* algorithms (or the key derivation function that combines them) need to be attacked in order to compromise the overall scheme.

2) *Dual Signatures*: A dual signature consists of two (or more) signatures. The signatures can be generated by two different algorithms using two secret keys. The dual signature is considered valid only if both of its signatures are valid.

It is possible to store a secondary (post-quantum) signature in a *non-critical* X.509 extension in a way that allows compatibility with existing Public Key Infrastructure (PKI) [22]. Current IETF efforts are directed towards “composite” dual certificates that do not use non-critical extensions [23].

D. Transport Layer Security (TLS)

Communication security and authentication mechanisms in IoT systems are currently largely based on lightweight TLS [24] stacks running on top of application protocols such as MQTT [25], [26]. Transition is still ongoing towards TLS protocol version 1.3 which was released in 2018.

Post-quantum transition only affects the asymmetric components of TLS 1.3; its symmetric authenticated encryption (AEAD) and key derivation components (cipher suites) readily support post-quantum levels from L1 to L5. New PQC algorithms are only used for key exchange and endpoint authentication, not for the transmission of bulk data streams.

TLS is a flexible, extensible protocol that negotiates the symmetric cipher suites, supported key establishment methods (“groups”), and authentication signature algorithms as part of its client-server handshake. New public-key algorithms can be fairly easily incorporated in the framework. Ad hoc post-quantum TLS implementations have existed at least since 2015 [27]. The Open Quantum Safe² project provides a free OpenSSL variant with support for a large subset of NIST algorithms [28]. In these implementations a NIST PQC KEM is used for key exchange and authentication is performed with a NIST PQC signature algorithm and certificates [29].

¹Dustin Moody (NIST), “Revising FAQ questions on hybrid modes”, October 30, 2019. https://groups.google.com/a/list.nist.gov/d/msg/pqc-forum/qRP63ucWlgs/rY5Sr_52AAAJ

²Open Quantum Safe Project: <https://openquantumsafe.org/>

E. The Cloud: Large-Scale PQC Experiments

The large-scale post-quantum cloud experiments ran by Amazon [30], Google [31], and Cloudflare [32] have focused on ephemeral hybrid key exchange methods in TLS (BoringSSL and S2N implementations). Algorithm selection in these experiments was limited to only one or two candidates, and focus was on networking performance; how the communication infrastructure copes with the changes introduced by the post-quantum transition.

Cloudflare and Google used NTRU variant HRSS-SXY [33], which has a relatively slow key generation phase and is therefore not ideally suited for ephemeral key exchange (potential key caching improves latency but not energy profile). They also experimented with isogeny-based proposal SIKE [34], which has the shortest messages but is computationally very expensive (slow). Google saw this experiment primarily as a comparison between isogeny-based systems and (structured) lattice schemes and tried to pick an “average” algorithm from the latter set. Google and Cloudflare consider HRSS as a more promising algorithm for TLS than SIKE [31], [32].

The Amazon system [30] currently supports SIKE [34] and BIKE [35] algorithms. Since both of these schemes are relatively new and quite inefficient, we assume that their selection was motivated solely by research interest; Amazon’s researchers are co-authors of both of these proposals.

In these experiments authentication (signatures) has been seen as a secondary consideration to key exchange (KEMs). This is a sensible approach while advanced quantum computers are not available; authentication occurs only in the present time but a weak key exchange method can be attacked at any point in the future, compromising session confidentiality. A practical problem in trialing post-quantum signatures for TLS is that there is no widespread Certification Authority (CA) or PKI support for PQC certificates currently available.

II. ENERGY MEASUREMENTS

NIST has adopted ARM Cortex M4 CPU [36] as their reference platform for lightweight PQC algorithm evaluation. Cortex M4 uses the ARMv7-m architecture, a somewhat stripped down version of ARM’s 32-bit ISA (Instruction Set Architecture). Cortex M4 is licensed by ARM as an IP core and is often implemented as a single-chip microcontroller (MCU SoC). Such Cortex M4 - based MCU chips typically cost less than \$10 and are manufactured by NXP, ST Microelectronics, Microchip/Atmel, and many others. Billions of units are shipped each year, mainly for consumer electronics, home appliances, industrial and automotive applications.

The PQM4³ project has helped to port many of the PQC candidate algorithms to the Cortex M4 target platform. Many of these implementations have target-specific assembly language optimizations created by the design teams for this purpose [37]. We use the same implementations in our benchmarking but with different testing firmware and platform. For reference, we also measured conventional NIST-curve ECDH

³PQM4 project, source code, and results: <https://github.com/mupq/pqm4>

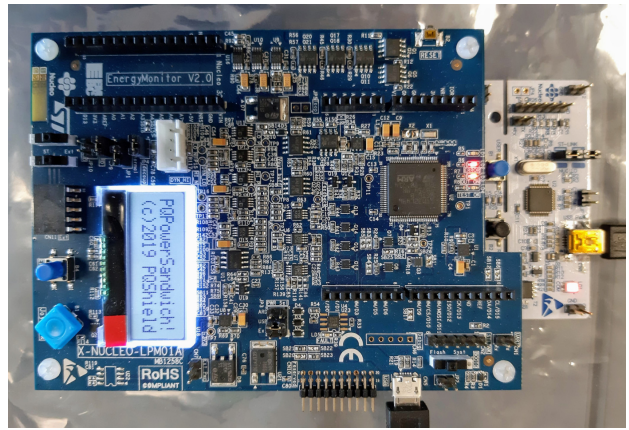


Fig. 1. The Post-Quantum Power Sandwich: The LPM01A “Power Shield” programmable power supply installed on top of a NUCLEO-F411RE target.

(key agreement) and ECDSA (signature) algorithms. The ECC implementation used is Ken MacKay’s “micro-ecc”.⁴

Note that ARM SecurCore SC300⁵ secure elements are based on a closely related ARMv6-m (Cortex M3) architecture. STMicroelectronics alone had shipped more than a billion SC300-based ST33 units by early 2019. These chips are widely used as (e)SIMs (Subscriber Identity Modules) and TPMs (Trusted Platform Modules). Cortex M4 implementations run on SC300 targets with only minor modifications and with very similar cycle counts. Cortex M4 performance is, therefore, a reasonable indicator for expected performance on real-life SIMs, TPMs, smart cards, and other secure elements if no PQC-specific cryptography acceleration is implemented. However additional software side-channel countermeasures are appropriate on these applications since their attack model includes physical attacks (PQM4 implementations only have some countermeasures against timing attacks).

A. PQPS, the Post-Quantum Power Sandwich

STMicroelectronics X-NUCLEO-LPM01A “PowerShield” [38] was used for our power measurements. PowerShield is an industry-standard power and energy measurement system adopted by the Ultra-Low Power (ULP) group of EEMBC⁶ for their ULPMark, IoTMark, and SecureMark benchmarks.

The target algorithms were run on a NUCLEO-F411RE development board. This particular STM32F411RE [39] Cortex M4 MCU has a maximum clock frequency of 100 MHz, 128 kBytes of SRAM and 512 kB of Flash memory. We chose this newer, but more limited board over STM32F407VG Discovery [40] (used by the PQM4 team) as it supports direct, external switched-mode power supply to the Vcore pin of the MCU, allowing power measurements with less interference

⁴micro-ecc: A small and fast ECDH and ECDSA implementation for 8-bit, 32-bit, and 64-bit processors. <https://github.com/kmackay/micro-ecc>

⁵SC300: <https://www.arm.com/products/silicon-ip-cpu/securcore/sc300>

⁶EEMBC, the Embedded Microprocessor Benchmark Consortium develops various embedded system benchmarks: <https://www.eembc.org/>

from peripherals. Several minor hardware modifications were necessary; these are documented on the project web site.

The PowerShield measurement board is designed to be installed on the top of the target board; hence the name “Post-Quantum Power Sandwich” (PQPS) for this experiment. Fig. 1 shows the system configuration. The PowerShield was running its default benchmarking firmware, while the target board was running the firmware that we developed. Python scripts control both boards simultaneously and collect results on a Ubuntu Linux 18.04 host.

We adopted most of the PQM4 [37] PQC implementations to work with our Mbed OS - based test firmware; ARM’s gcc-based cross compilers and assemblers were used. See Table I for a list of supported algorithms. We tried to add as many of the NIST PQC candidate algorithms in our testing suite as possible and will continue to update it. Many of the excluded algorithms simply do not fit on the target IoT platform due to excessive computational or memory requirements. All source code and scripts used in the PQPS experiment is open source and available from: <https://github.com/mjosaarinen/pqps>.

B. Measurement Results

Table II summarizes our results. Some NIST-curve ECDH and ECDSA measurements are offered as a reference; For PQC algorithms the table contains the claimed post-quantum security level L1 ··· L5 [13], followed by public key (PubKey), ciphertext (CphTxt) and signature (SigLen) lengths in bytes and the actual measurements for keypair generation, encapsulation, decapsulation (corresponding to public-key encryption and decryption), and creating and verifying signatures. Each measurement consists of timing in millions of clock cycles, average power in milliwatts, and energy in Joules.

The MCU was clocked at 96 MHz during the experiment. The PowerShield was programmed to regulate the voltage at 3.00 V and integrate energy consumption from dynamic current (which the device samples with high frequency). The current varied between 10.6 mA and 37.8 mA during acquisition. The on-board temperature sensor reported between 20.0 °C and 27.0 °C during the experiment, with 78 % of measurements at $26 \pm 1^\circ\text{C}$. The temperature stayed within 5 °C from each board self-calibration.

Each acquisition was synchronized with the execution of the target algorithm at microsecond precision by using one of the interface pins (d7) as a trigger (a feature of PowerShield firmware). Each measurement ran for 10 000 ms (roughly 10^9 cycles) which is usually sufficient for hundreds of iterations; average Wattage was derived from this measurement. The target board itself performed clock cycle counts; the energy usage of each primitive is derived from these quantities.

We performed at least three full runs of all algorithm measurements and randomized the order in each run. This required several days of non-stop automated testing. The three results (which themselves are averages of thousands of individual measurements) were verified to have satisfactory consistency and precision.

For additional implementation metrics such as code size and stack usage, we refer the reader to the PQM4 project [37] since we used largely the same implementations.

a) Note on SIKE Measurements and Implementations:

Unlike other algorithms SIKE may require more than 10 seconds for a single operation. The overall energy consumption is extrapolated from the power draw during the first 10 seconds; its instruction mix and power draw seems to be quite homogeneous during algorithm execution, however. Faster implementations of SIKE for Cortex M4 in assembly language are reported in [41], but these implementations have not been made publicly available for measurement. Reported cycle counts indicate that these are still about 100 times slower than lattice-based schemes at the same PQ security level. On slower CPUs their multi-second latency can severely affect usability in addition to the energy budget.

C. On PC and Server-side Energy Consumption

We also measured the energy consumption of PQC algorithms on PC-class laptop and desktop targets. This experiment instrumented the SUPERCOP benchmarking platform with Intel’s built-in RAPL (Running Average Power Limit) energy counters and is available under the PQPS repository.⁷

We profiled 159 variants of 20 NIST PQC algorithms on typical desktop (i7-8700) and laptop (i5-8250U) systems. Three different components of each algorithm were measured separately, bringing the total number to several hundred; the experiment ran for many days even though the number of compiler options in SUPERCOP was minimized.

The average energy was $5.4 \text{ nJ}/\text{cycle}$ on the laptop system and $8.8 \text{ nJ}/\text{cycle}$ on the desktop system. The main observation was that power has relatively little variation depending on the algorithm in question on these platforms, being concentrated in a $\pm 10\%$ range (Fig. 2). These measurements, and the ones reported in [42] indicate that timing (cycle counts without related power measurements) leads to reasonable energy estimates on higher-end CPUs where power dissipation is more constant.

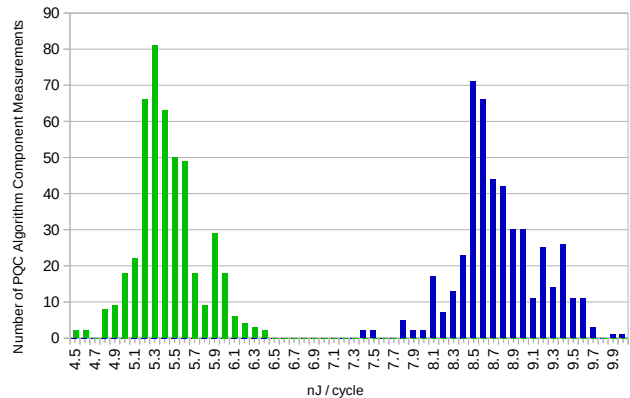


Fig. 2. Running power is much less algorithm-dependent on PC-class chips. Blue: i7-8700 @ 4.6 GHz (Desktop) Green: i5-8250U @ 3.4 GHz (Laptop)

⁷ SUPPERCOP: <https://github.com/mjosaarinen/pqps/tree/master/suppercop>

TABLE II
BANDWIDTH, CPU CYCLE, POWER, AND ENERGY USAGE OF PQC ALGORITHMS ON CORTEX M4 STM32F AT 96 MHZ

Key Establishment Algorithm / Variant	PQ Level	Transmit Bytes		Keypair Generation			Encapsulate			Decapsulate		
		PubKey	CphTxt	10 ⁶ clk	mW	Energy	10 ⁶ clk	mW	Energy	10 ⁶ clk	mW	Energy
ECDH-secp256k1	none	64	64	4.108	65.41	2.799 mJ	8.215	65.36	5.594 mJ	4.108	65.45	2.801 mJ
ECDH-secp256r1	none	64	64	5.814	60.47	3.663 mJ	11.63	59.99	7.267 mJ	5.815	60.35	3.656 mJ
FrodoKEM-640-AES	[L1]	9616	9720	48.38	73.96	37.28 mJ	47.20	71.34	35.08 mJ	46.65	71.04	34.52 mJ
...-640-SHAKE	[L1]	9616	9720	80.01	79.03	65.87 mJ	80.00	77.92	64.94 mJ	79.44	77.84	64.42 mJ
Kyber512	[L1]	800	736	0.516	76.88	413.6 μ J	0.654	78.33	534.0 μ J	0.623	78.28	508.8 μ J
Kyber768	[L3]	1184	1088	0.978	75.77	772.3 μ J	1.150	76.80	920.4 μ J	1.100	76.50	876.3 μ J
Kyber1024	[L5]	1568	1568	1.575	77.11	1.265 mJ	1.784	77.61	1.442 mJ	1.714	77.47	1.383 mJ
NewHope512-CCA	[L1]	928	1120	0.591	78.52	483.9 μ J	0.922	78.09	750.1 μ J	0.906	77.77	734.0 μ J
NewHope1024-CCA	[L5]	1824	2208	1.167	78.91	959.3 μ J	1.785	78.31	1.456 mJ	1.764	78.13	1.436 mJ
NTRU-HPS2048509	[L1]	699	699	78.79	41.94	34.42 mJ	0.634	59.89	395.6 μ J	0.546	84.20	479.6 μ J
NTRU-HPS2048677	[L3]	930	930	141.3	41.18	60.62 mJ	0.943	59.30	582.7 μ J	0.849	83.52	739.0 μ J
NTRU-HRSS701	[L3]	1138	1138	154.2	41.18	66.15 mJ	0.398	79.25	328.8 μ J	0.898	82.91	776.0 μ J
NTRU-HPS4096821	[L5]	1230	1230	212.0	40.90	90.31 mJ	1.189	59.02	731.0 μ J	1.079	84.49	949.6 μ J
R5ND_1KEM_5d	[L1]	445	565	0.342	73.76	263.5 μ J	0.544	71.82	407.1 μ J	0.729	69.47	527.9 μ J
R5ND_3KEM_5d	[L3]	780	883	0.675	70.20	493.9 μ J	1.015	70.90	749.4 μ J	1.298	69.89	945.3 μ J
R5ND_5KEM_5d	[L5]	972	1095	1.229	66.42	850.0 μ J	1.785	66.00	1.227 mJ	2.339	64.47	1.571 mJ
R5N1_1KEM_0d	[L1]	5214	5252	5.577	55.63	3.232 mJ	4.487	65.57	3.065 mJ	5.340	65.61	3.650 mJ
R5N1_3KEM_0d	[L3]	8834	8890	8.914	54.53	5.063 mJ	7.416	64.56	4.987 mJ	8.445	65.19	5.735 mJ
R5N1_5KEM_0d	[L5]	14264	14320	32.82	60.90	20.82 mJ	21.88	59.74	13.62 mJ	25.59	60.37	16.10 mJ
LightSaber	[L1]	672	736	0.457	82.50	393.2 μ J	0.651	82.41	559.3 μ J	0.677	83.23	587.8 μ J
Saber	[L3]	992	1088	0.899	82.32	771.2 μ J	1.170	82.71	1.008 mJ	1.209	83.44	1.051 mJ
FireSaber	[L5]	1312	1472	1.455	81.87	1.241 mJ	1.791	82.20	1.533 mJ	1.854	82.63	1.596 mJ
LAC128	[L1]	544	712	2.275	49.61	1.176 mJ	3.993	49.11	2.043 mJ	6.064	50.58	3.195 mJ
LAC192	[L3]	1056	1188	7.546	49.81	3.916 mJ	10.01	50.53	5.267 mJ	18.53	50.23	9.698 mJ
LAC256	[L5]	1056	1424	7.686	50.94	4.079 mJ	13.56	50.66	7.158 mJ	22.22	50.59	11.71 mJ
BabyBear	[L2]	804	917	0.657	71.04	486.7 μ J	0.825	69.60	598.8 μ J	1.276	68.06	904.5 μ J
MamaBear	[L4]	1194	1307	1.280	70.58	941.4 μ J	1.501	69.33	1.084 mJ	2.137	68.21	1.518 mJ
PapaBear	[L5]	1584	1697	2.126	70.16	1.554 mJ	2.400	69.16	1.729 mJ	3.232	68.28	2.299 mJ
ntrupr653	[L2]	897	1025	56.57	47.06	27.73 mJ	112.6	47.07	55.24 mJ	168.4	47.09	82.59 mJ
ntrupr761	[L3]	1039	1167	76.64	47.74	38.12 mJ	152.7	47.87	76.14 mJ	228.3	47.23	112.3 mJ
ntrupr857	[L4]	1184	1312	97.03	47.13	47.64 mJ	193.3	47.25	95.16 mJ	289.2	47.11	141.9 mJ
sntrup653	[L2]	994	897	600.3	46.38	290.1 mJ	56.68	47.76	28.21 mJ	171.4	46.69	83.34 mJ
sntrup761	[L3]	1158	1039	813.4	46.32	392.5 mJ	76.76	47.32	37.84 mJ	232.4	46.49	112.6 mJ
sntrup857	[L4]	1322	1184	1027	46.69	499.5 mJ	97.16	48.05	48.63 mJ	293.9	46.20	141.4 mJ
SIKEp434	[L1]	330	346	666.0	67.89	471.0 mJ	1091	68.18	774.7 mJ	1163	68.17	826.1 mJ
SIKEp503	[L2]	378	402	1004	68.69	718.8 mJ	1656	68.81	1.187 J	1761	69.01	1.266 J
SIKEp610	[L3]	462	486	1880	68.72	1.346 J	3460	69.11	2.491 J	3480	69.10	2.505 J
SIKEp751	[L5]	564	596	3404	67.76	2.403 J	5521	68.40	3.934 J	5930	68.59	4.237 J

Signature Algorithm / Variant	PQ Level	Transmit Bytes		Keypair Generation			Sign			Verify		
		PubKey	SigLen	10 ⁶ clk	mW	Energy	10 ⁶ clk	mW	Energy	10 ⁶ clk	mW	Energy
ECDSA-secp256k1	none	64	64	4.109	64.02	2.741 mJ	4.475	64.96	3.028 mJ	4.546	65.00	3.078 mJ
ECDSA-secp256r1	none	64	64	5.814	59.14	3.582 mJ	6.185	59.97	3.864 mJ	6.639	59.88	4.142 mJ
Dilithium2	[L1]	1184	2044	1.328	77.58	1.073 mJ	4.663	77.75	3.777 mJ	1.389	77.49	1.121 mJ
Dilithium3	[L2]	1472	2701	2.172	77.78	1.760 mJ	7.212	76.48	5.746 mJ	2.116	77.37	1.705 mJ
Dilithium4	[L3]	1760	3366	2.930	78.25	2.389 mJ	7.263	77.11	5.834 mJ	2.997	78.02	2.436 mJ
Falcon-512	[L1]	897	690	182.2	62.53	118.7 mJ	39.57	55.91	23.05 mJ	0.493	67.12	345.0 μ J
Falcon-512-tree	[L1]	897	690	200.9	62.31	130.4 mJ	18.19	60.18	11.40 mJ	0.492	66.80	342.7 μ J
Falcon-1024	[L5]	1793	1330	380.2	58.72	232.6 mJ	79.36	54.67	45.19 mJ	1.013	65.37	690.0 μ J

III. ANALYSIS AND DISCUSSION

Most microchip technology follows the MOSFET / CMOS “dynamic power equation” [43] which can be written as

$$P_{\text{dyn}} = \alpha \cdot C \cdot V^2 \cdot f. \quad (1)$$

Here P_{dyn} = Dynamic power, α = activity, C = Capacitive load, V = Voltage, and f = Frequency. Only the activity variable α depends on the particular instruction mix being executed. CPUs, of course, have also static power consumption; ultra-low power CPUs a lot less (by design) than desktop CPUs.

Since frequency f has a linear relationship with power (Eqn. 1) and cycle length $1/f$ with algorithm execution time,

frequency mostly cancels out and has surprisingly little effect on the energy consumption of individual algorithms at CPUs “efficiency range”. However at very high frequencies (flash program) memory or other components may introduce additional wait states forcing algorithms to use up more clock cycles for the same task. Higher clock frequencies may also require higher voltage (voltage scaling); note the V^2 term.

Estimation on other targets can be performed via relative Wattage, cycles, and a platform scaling parameter that is often expressed in $\mu A/\text{MHz}$. Product datasheets often contain vague or misleading values for this quantity; we recommend careful calibration with some benchmark algorithm [44].

A. Effect of Key and Ciphertext Lengths

In addition to energy consumed by computation, the length of public keys, signatures, and ciphertext also affect the energy consumption via increased radio communication. Significantly reduced transmission energy and time has traditionally been seen as the most important advantage of ECC over RSA. We can use RSA public key and ciphertext (or signature) lengths as a yardstick for bandwidth requirements.

The bandwidth requirements of the PQC candidate with the shortest ciphertexts and public keys, Isogeny-based SIKEp434 [34] corresponds to RSA with 2600-bit keys, while the most efficient lattice-based proposal Round5 (R5ND_1KEM_5d) [46] corresponds to RSA with 4000-bit keys at the same post-quantum security level. However, Round5 and other structure lattice schemes require less than one percent of the computation time and energy of SIKE.

We observe that the per-bit transmission energy e_{xfer} has dropped from $10\mu\text{J}/\text{bit}$ during the 2G (EDGE) era to less than $1.0\mu\text{J}/\text{bit}$ for mobile device WiFi, HSPA, Bluetooth LE, ZigBee, and LTE (See Fig. 3) [45], [47]. Currently $0.1\mu\text{J}/\text{bit}$ can be expected with LTE or with Bluetooth LE technologies. Predicted 5G transmission speeds imply e_{xfer} in nJ/bit range.

Simple estimation models for total energy can be used to choose an appropriate algorithm depending on e_{xfer} :

$$\begin{aligned} E_{\text{KG}} &+ e_{\text{xfer}}|\text{pubkey}| && \text{for key generation,} \\ E_{\text{Enc}} &+ e_{\text{xfer}}|\text{ciphertext}| && \text{for encapsulation,} \\ E_{\text{Sign}} &+ e_{\text{xfer}}|\text{signature}| && \text{for authentication.} \end{aligned}$$

where E_{KG} , E_{Enc} , and E_{Sign} are the energy required for computation of keypairs, encapsulation, and signatures and vertical bars indicate data length in bits.

The relevant “energy basket” depends on the particular protocol and communicating party (Alice or Bob?). We can also construct generalized “index” energy baskets for the purpose of comparing algorithms. For example

$$E_{\text{KG}} + E_{\text{Enc}} + E_{\text{Dec}} + e_{\text{xfer}}(|\text{pubkey}| + |\text{ciphertext}|) \quad (2)$$

estimates the *total* energy of an ephemeral key exchange; in this case e_{xfer} is the total energy to send (and receive) a bit.

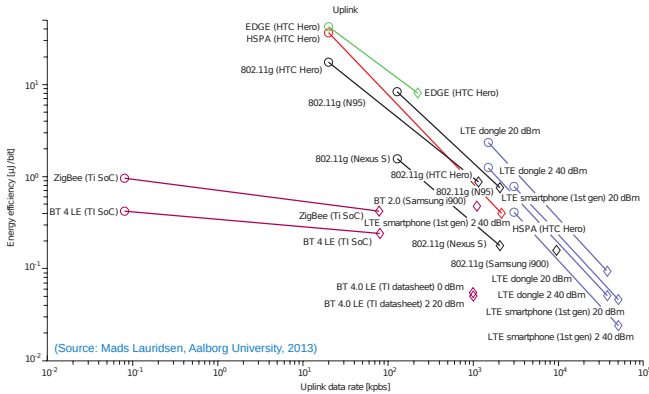


Fig. 3. Transmission efficiency in the pre-5G era. From Lauridsen et al [45].

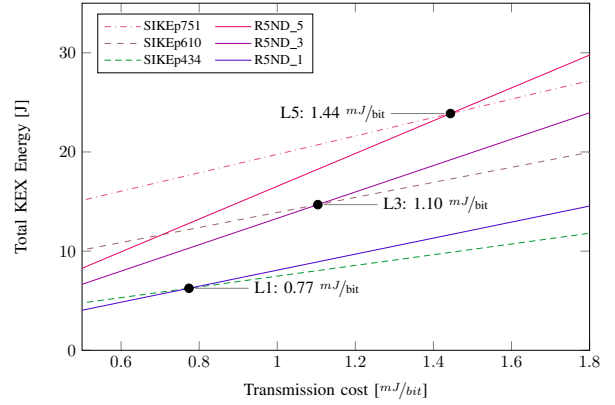


Fig. 4. Energy cross-over from Round5 to SIKE is around $> 1 \text{ mJ}/\text{bit}$.

B. Transmission Energy Cross-over Points

When other relevant engineering factors are fixed and algorithm selection depends on transmission energy alone, we may use an energy model or “basket” such as Equation 2 to determine rough (order of magnitude) cross-over points for energy-optimal algorithm selection.

Based on our data, the smaller message length of Isogeny-based PQC justifies its energy consumption over structured lattices when transmission energy is above the magnitude of $e_{\text{xfer}} > 1 \text{ mJ}/\text{bit}$ (Fig. 4), hundreds of times higher than e_{xfer} of common radio interface technologies used today [45].⁸

We may also determine the cross-over point from structured lattices to conventional ECC cryptography. Our data indicates ECDHE to be more energy-efficient when $e_{\text{xfer}} > 1 \mu\text{J}/\text{bit}$. Actual cross-over estimates for Round5 are 1.9/2.7/3.2 $\mu\text{J}/\text{bit}$ for 256/384/512-bit EC curves (equivalent to 128/192/256-bit or L1/L3/L5 classical security – but no PQ security).

IV. CONCLUSIONS

We find that post-quantum transition can imply energy savings over current ECC cryptography even with current radio technologies, and increasingly more with 5G’s transmission speeds. Some existing ECC use cases will remain that can’t readily support longer messages of any of the PQC alternatives (or RSA) but for TLS it is not a problem. Furthermore, there is a huge scale in PQC energy requirements (Fig. 5).

Adam Langley (Google) concludes observations from Google / Cloudflare post-quantum cloud experiment [31] as

... Thus the overall conclusion of these experiments is that post-quantum confidentiality in TLS should probably be based on structured lattices ...

Our IoT experiments support this view. Here “structured lattices” refers to cryptosystems based on NTRU, RLWE, and related problems. The comparison was made against Isogeny-based PQC cryptography (SIKE) in particular.

⁸Transmission energy of $e_{\text{xfer}} > 1 \text{ mJ}/\text{bit}$ implies either continuous RF transmission power of several Watts (requiring a radio license) or data rate of just hundreds of bits per second. Battery life is low if there is any kind of data payload; 5 megabytes will completely drain a 40 kJ smartphone battery.

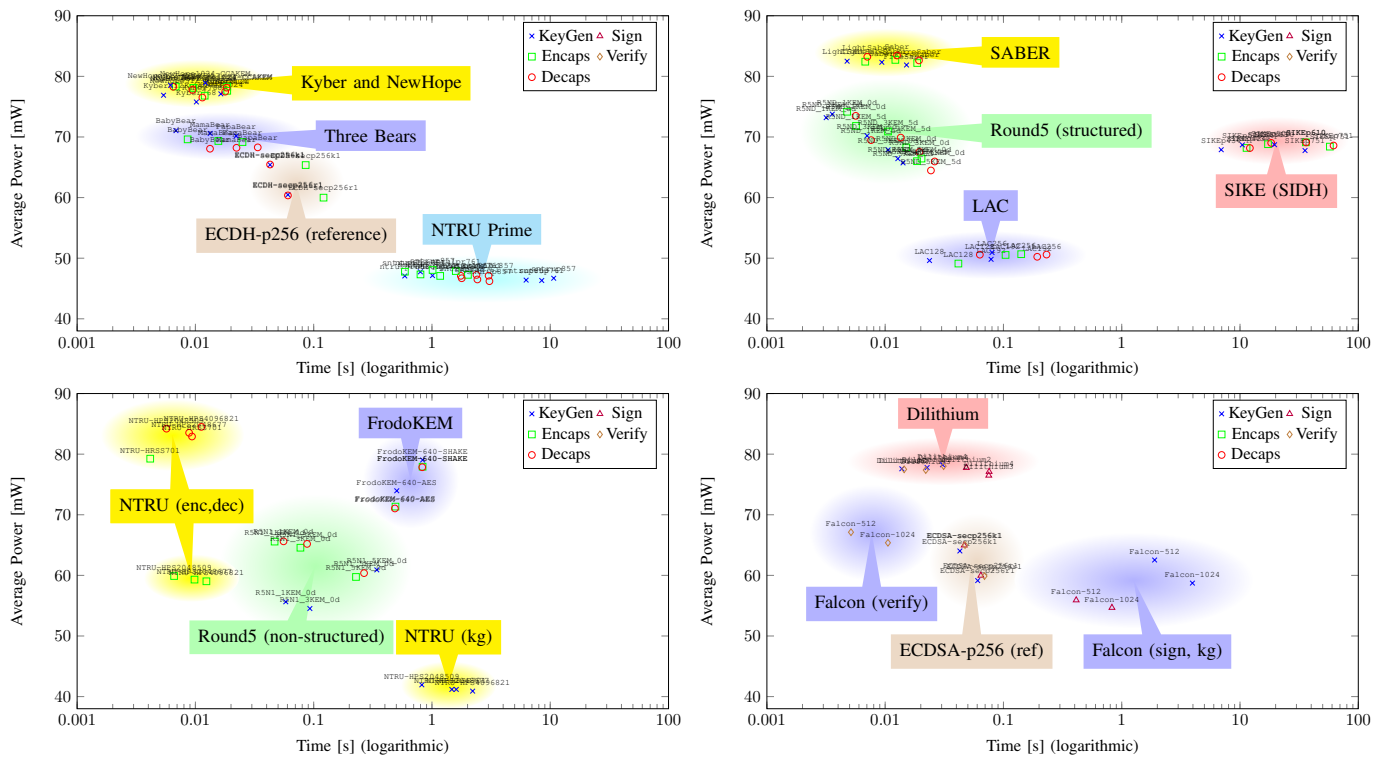


Fig. 5. The average power of the Cortex M4 target (STM32F411RE at 96 MHz) varies significantly depending on the algorithm – from 40 mW to 85 mW – but computation time has a scale of four orders of magnitude. All security levels of the same algorithm usually fit into the same cluster since the time axis is logarithmic. Note how some algorithms such as NTRU and Falcon have significantly more complex key generation than other operations.

Kyber, NewHope, Round5, and Saber have lightweight variants where all three primitive operations < 1 mJ and public key size and ciphertext expansion is bound by approximately one kilobyte (NewHope slightly more). Additionally LAC and ThreeBears are very close and are faster than ECC. NTRU (HRSS) has a computationally expensive keypair generation which limits its usability in the ephemeral (forward secure) TLS use case. The NTRU Prime variant is much slower than NTRU; not all “structured lattice” algorithms are equivalent.

The Dilithium and Falcon lattice-based signature algorithms are suitable for mobile devices and PKI as also noted in [48]. Falcon has smaller public keys, signatures, and faster signature verification so it would be preferred for client-side applications (i.e. when the mobile device verifies server certificates but does not sign). The signature performance of Falcon suffers from a lack of a double-precision floating point unit on our test platform, however, so Dilithium may be preferable when both parties are expected to use certificate-based authentication.

REFERENCES

- [1] P. W. Shor, “Algorithms for quantum computation: Discrete logarithms and factoring,” in *Proc. FOCS '94*. IEEE, 1994, pp. 124–134. [Online]. Available: <https://arxiv.org/abs/quant-ph/9508027>
- [2] ECRYPT, “PQCrypto 2006: International workshop on post-quantum cryptography,” May 2006, workshop Record. [Online]. Available: <https://postquantum.cr.yp.to/pqcrypto2006record.pdf>
- [3] G. Alagic, J. Alperin-Sheriff, D. Apon, D. Cooper, Q. Dang, C. Miller, D. Moody, R. Peralta, R. Perlner, A. Robinson, D. Smith-Tone, and Y.-K. Liu, “Status report on the first round of the nist post-quantum cryptography standardization process,” NISTIR 8240, January 2019. [Online]. Available: <https://nvlpubs.nist.gov/nistpubs/ir/2019/NIST.IR.8240.pdf>
- [4] L. Chen, S. Jordan, Y.-K. Liu, D. Moody, R. Peralta, R. Perlner, and D. Smith-Tone, “Report on post-quantum cryptography,” NISTIR 8105, April 2016. [Online]. Available: <https://nvlpubs.nist.gov/nistpubs/ir/2016/NIST.IR.8105.pdf>
- [5] NCSA, “Quantum key distribution,” November 2016, white Paper published by UK National Cyber Security Centre. [Online]. Available: <https://www.ncsc.gov.uk/whitepaper/quantum-key-distribution>
- [6] CNSS, “Use of public standards for the secure sharing of information among national security systems,” Committee on National Security Systems: CNSS Advisory Memorandum, CNSSAM 02-15, July 2015.
- [7] NSA/CSS, “Commercial national security algorithm suite,” August 2015. [Online]. Available: <https://apps.nsa.gov/iaarchive/programs/iad-initiatives/cnsa-suite.cfm>
- [8] M. Pecen and et al., “Quantum safe cryptography and security: An introduction, benefits, enablers and challenges,” June 2015, eTSI White Paper No. 8. [Online]. Available: <https://www.etsi.org/images/files/ETSIWhitePapers/QuantumSafeWhitepaper.pdf>
- [9] R. A. Perlner and D. A. Cooper, “Quantum resistant public key cryptography: a survey,” in *IDTrust 2009*, ser. ACM International Conference Proceeding Series, K. E. Seamons, N. McBurnett, and T. Polk, Eds. ACM, 2009, pp. 85–93. [Online]. Available: https://tsapps.nist.gov/publication/get_pdf.cfm?pub_id=901595
- [10] J. Nechvatal, E. Barker, L. Bassham, W. Burr, M. Dworkin, J. Foti, and E. Roback, “Report on the development of the advanced encryption standard (AES),” *Journal of Research of the National Institute of Standards and Technology*, vol. 106, no. 3, pp. 511–577, May-June 2001. [Online]. Available: <https://nvlpubs.nist.gov/nistpubs/jres/106/3/j63nec.pdf>
- [11] S.-J. Chang, R. Perlner, W. E. Burr, M. S. Turan, J. M. Kelsey, S. Paul, and L. E. Bassham, “Third-round report of the SHA-3 cryptographic hash algorithm competition,” NISTIR 7896, November 2012. [Online]. Available: <https://nvlpubs.nist.gov/nistpubs/ir/2012/NIST.IR.7896.pdf>

- [12] NIST, Ed., *Round 2 submissions to the NIST PQC Project*, March 2019. [Online]. Available: <https://csrc.nist.gov/Projects/Post-Quantum-Cryptography/Round-2-Submissions>
- [13] NIST, "Submission requirements and evaluation criteria for the post-quantum cryptography standardization process," Official Call for Proposals, National Institute for Standards and Technology, December 2016. [Online]. Available: <http://csrc.nist.gov/groups/ST/post-quantum-crypto/documents/call-for-proposals-final-dec-2016.pdf>
- [14] R. Cramer and V. Shoup, "Design and analysis of practical public-key encryption schemes secure against adaptive chosen ciphertext attack," *SIAM Journal on Computing*, vol. 33, no. 1, pp. 167–226, 2003. [Online]. Available: <http://www.shoup.net/papers/cca2.pdf>
- [15] N. Unger and I. Goldberg, "Improved strongly deniable authenticated key exchanges for secure messaging," *PoPETS*, vol. 2018, no. 1, pp. 21–66, 2018. [Online]. Available: <https://doi.org/10.1515/popets-2018-0003>
- [16] L. K. Grover, "A fast quantum mechanical algorithm for database search," in *Proceedings of the Twenty-eighth Annual ACM Symposium on Theory of Computing*, ser. STOC '96. ACM, 1996, pp. 212–219. [Online]. Available: <http://arxiv.org/abs/quant-ph/9605043>
- [17] A. Chailloux, M. Naya-Plasencia, and A. Schrottenloher, "An efficient quantum collision search algorithm and implications on symmetric cryptography," in *ASIACRYPT 2017 (2)*, ser. LNCS, T. Takagi and T. Peyrin, Eds., vol. 10625. Springer, 2017, pp. 211–240. [Online]. Available: <https://eprint.iacr.org/2017/847>
- [18] E. Barker, L. Chen, A. Roginsky, A. Vassilev, and R. Davis, "Recommendation for pair-wise key establishment schemes using discrete logarithm cryptography," NIST Special Publication SP 800-56A, Revision 3, April 2018. [Online]. Available: <https://nvlpubs.nist.gov/nistpubs/SpecialPublications/NIST.SP.800-56Ar3.pdf>
- [19] E. Barker, L. Chen, A. Roginsky, A. Vassilev, R. Davis, and S. Simon, "Recommendation for pair-wise key establishment using integer factorization cryptography," NIST Special Publication SP 800-56B, Revision 2, March 2019. [Online]. Available: <https://nvlpubs.nist.gov/nistpubs/SpecialPublications/NIST.SP.800-56Br2.pdf>
- [20] FIPS, "(FIPS) 186-4, digital signature standard (DSS)," Federal Information Processing Standards Publication, July 2013. [Online]. Available: <https://nvlpubs.nist.gov/nistpubs/FIPS/NIST.FIPS.186-4.pdf>
- [21] C. Peikert, "A decade of lattice cryptography," *Foundations and Trends in Theoretical Computer Science*, vol. 10, no. 4, pp. 283–424, 2016. [Online]. Available: <https://eprint.iacr.org/2015/939>
- [22] P. Kampanakis, P. Panburana, E. Daw, and D. V. Geest, "The viability of post-quantum x.509 certificates," IACR ePrint 2018/063, January 2018. [Online]. Available: <https://eprint.iacr.org/2018/063>
- [23] M. Ounsworth, "Composite keys and signatures for use in internet PKI," IETF Internet-Draft, July 2019. [Online]. Available: <https://tools.ietf.org/html/draft-ounsworth-pq-composite-sigs>
- [24] E. Rescorla, "The Transport Layer Security (TLS) protocol version 1.3," IETF RFC 8446, August 2018. [Online]. Available: <https://tools.ietf.org/html/rfc8446>
- [25] A. Banks, E. Briggs, K. Borgendale, and R. Gupta, "MQTT version 5.0," March 2019. [Online]. Available: <https://docs.oasis-open.org/mqtt/mqtt/v5.0/os/mqtt-v5.0-os.pdf>
- [26] G. Brown and L.-P. Lamoureux, "MQTT and the NIST cybersecurity framework version 1.0," May 2014. [Online]. Available: <http://docs.oasis-open.org/mqtt/mqtt-nist-cybersecurity/v1.0/cn01/mqtt-nist-cybersecurity-v1.0-cn01.pdf>
- [27] J. W. Bos, C. Costello, M. Naehrig, and D. Stebila, "Post-quantum key exchange for the TLS protocol from the ring learning with errors problem," in *IEEE S & P 2015*. IEEE Computer Society, 2015, pp. 553–570, extended version available as IACR ePrint 2014/599. [Online]. Available: <https://eprint.iacr.org/2014/599>
- [28] D. Stebila and M. Mosca, "Post-quantum key exchange for the internet and the open quantum safe project," in *SAC 2016*, ser. LNCS, R. Avanzi and H. M. Heys, Eds., vol. 10532, 2016, pp. 14–37. [Online]. Available: <https://eprint.iacr.org/2016/1017>
- [29] E. Crockett, C. Paquin, and D. Stebila, "Prototyping post-quantum and hybrid key sxchange and authentication in TLS and SSH," IACR ePrint 2019/858, July 2019. [Online]. Available: <https://eprint.iacr.org/2019/858>
- [30] A. Hopkins, "Post-quantum TLS now supported in AWS KMS," November 2019, blog posting related to Amazon Web Services. [Online]. Available: <https://aws.amazon.com/blogs/security/post-quantum-tls-now-supported-in-aws-kms/>
- [31] A. Langley, "Real-world measurements of structured-lattices and supersingular isogenies in TLS," October 2019, blog posting related to Google Chrome. [Online]. Available: <https://www.imperialviolet.org/2019/10/30/pqsivssl.html>
- [32] K. Kwiatkowski and L. Valenta, "The TLS post-quantum experiment," October 2019, blog posting related to Cloudflare servers. [Online]. Available: <https://blog.cloudflare.com/the-tls-post-quantum-experiment/>
- [33] T. Saito, K. Xagawa, and T. Yamakawa, "Tightly-secure key-encapsulation mechanism in the quantum random oracle model," in *EUROCRYPT 2018 (3)*, ser. LNCS, J. B. Nielsen and V. Rijmen, Eds., vol. 10822. Springer, 2018, pp. 520–551. [Online]. Available: <https://eprint.iacr.org/2017/1005>
- [34] D. Jao, R. Azarderakhsh, M. Campagna, C. Costello, L. D. Feo, B. Hess, A. Jalali, B. Koziel, B. LaMacchia, P. Longa, M. Naehrig, J. Renes, V. Soukharev, D. Urbanik, and G. Pereira, "SIKE," NIST, Ed., March 2019. [Online]. Available: <https://csrc.nist.gov/Projects/Post-Quantum-Cryptography/Round-2-Submissions>
- [35] N. Aragon, P. Barreto, S. Betteieb, L. Bidoux, O. Blazy, J.-C. Deneuville, P. Gaborit, S. Gueron, T. Guney, C. A. Melchor, R. Misoczki, E. Persichetti, N. Sendrier, J.-P. Tillich, G. Zemor, and V. Vasseu, "BIKE," Round 2 submission to the NIST PQC Project, March 2019. [Online]. Available: <https://csrc.nist.gov/Projects/Post-Quantum-Cryptography/Round-2-Submissions>
- [36] ARM, "ARM Cortex-M4 processor, technical reference manual," ARM 100166_0001_00_en, Revision r0p1, 2015. [Online]. Available: http://infocenter.arm.com/help/topic/com.arm.doc.100166_0001_00_en/arm_cortexm4_processor_trm_100166_0001_00_en.pdf
- [37] M. J. Kannwischer, J. Rijneveld, P. Schwabe, and K. Stoffelen, "pqm4: Testing and benchmarking nist pqc on arm cortex-m4," Presented in the second NIST PQC Standardization Workshop, August 2019. IACR ePrint 2019/844, July 2019. [Online]. Available: <https://eprint.iacr.org/2019/844>
- [38] STMicroelectronics, "STM32 Nucleo expansion board for power consumption measurement," User manual UM2243, March 2018. [Online]. Available: https://www.st.com/resource/en/user_manual/dm00406577.pdf
- [39] —, "STM32F411xC STM32F411xE," Production Datasheet, December 2017. [Online]. Available: <https://www.st.com/resource/en/datasheet/stm32f411re.pdf>
- [40] —, "Discovery kit with STM32F407VG MCU," Data Brief STM32F4DISCOVERY, October 2016. [Online]. Available: https://www.st.com/resource/en/data_brief/stm32f4discovery.pdf
- [41] H. Seo, A. Jalali, and R. Azarderakhsh, "SIKE round 2 speed record on ARM Cortex-M4," IACR ePrint 2019/535, May 2019. [Online]. Available: <https://eprint.iacr.org/2019/535>
- [42] C. A. Roma, C.-E. A. Tai, and M. A. Hasan, "Energy consumption of round 2 submissions for NIST PQC standards," Technical Report CACR 2019-03. Also presented at the Second NIST PQC Standardization Workshop, August 2019., University of Waterloo, Tech. Rep., 2019. [Online]. Available: <http://cacr.uwaterloo.ca/techreports/2019/cacr2019-03.pdf>
- [43] J. L. Hennessy and D. A. Patterson, *Computer Architecture, 6th Edition: A Quantitative Approach*. Morgan Kaufmann, 2019.
- [44] STMicroelectronics, "Accurate power consumption estimation for STM32L1 series of ultra-low-power microcontrollers," Technical Article TA0342, May 2013. [Online]. Available: https://www.st.com/resource/en/technical_article/dm00024152.pdf
- [45] M. Lauridsen, L. Noë, T. B. Sørensen, and P. Mogensen, "An empirical LTE smartphone power model with a view to energy efficiency evolution," *Intel Technology Journal*, vol. 18, no. 1, pp. 172–193, 2014.
- [46] O. Garcia-Morchon, Z. Zhang, S. Bhattacharya, R. Rietman, L. Tolhuizen, J.-L. Torre-Arce, H. Baan, M.-J. O. Saarinen, S. Fluhrer, T. Laarhoven, and R. Player, "Round5," Round 2 submission to the NIST PQC Project, March 2019. [Online]. Available: <https://csrc.nist.gov/Projects/Post-Quantum-Cryptography/Round-2-Submissions>
- [47] M. Lauridsen, "Studies on mobile terminal energy consumption for LTE and future 5G," Ph.D. dissertation, Aalborg University, November 2014. [Online]. Available: https://vbn.aau.dk/ws/portalfiles/portal/206141678/master_Lauridsen.pdf
- [48] P. Kampanakis and D. Sikeridis, "Two PQ signature use-cases: Non-issues, challenges and potential solutions." Presented at the 7th ETSI/IQC Quantum Safe Cryptography Workshop 2019. IACR ePrint 2016/030, November 2019. [Online]. Available: <https://eprint.iacr.org/2019/1276>